INFLUENCE OF MICROSTRUCTURE ON THE NON-OHMIC BEHAVIOR OF ZINC OXIDE VARISTOR CERAMICS PREPARED BY DIRECT MIXING OF CONSTITUENT PHASES

Akinnifesi, J. O.; Erinfolami, F. B. and Akinwunmi, O. O.
Department of Physics (Engineering Physics), Obafemi Awolowo University, Ile-Ife, Nigeria
(Corresponding Author: jakinnife@yahoo.com)
(Receive: 10th Feb., 2014: Accepted: 12th March, 2014)

ABSTRACT

Well ground powders of zinc oxide sample were doped with mixtures of 2% MnO_2 3% PbO and 3% MnO_2, 2% PbO. These were pressed and sintered at temperatures from 750°C to 850°C from different times from 12 to 42 hours, to diversify the microstructures of the resulting varistors. Grain sizes and distribution of phases were examined by the use of scanning electron microscope (SEM) and x-ray diffraction (XRD) techniques. Non-ohmic properties were obtained from the electrical field – current density characteristics. These were related to the microstructural properties. Experimental findings revealed that smaller grain sizes corresponded to higher non-linearity coefficients and breakdown fields. The barrier formation mechanisms were proposed as responsible for the microstructure-controlled non-ohmic behavior of the varistor samples.

Keywords : ZnO Ceramics, Varistor, Microstructure, Non-ohmic Properties, Electrical Characteristics

INTRODUCTION

Varistors are electronic devices having an extremely high resistance at low voltages and very low resistance at high voltages. They are characterized by a threshold voltage VT of non-linearity in their current –voltage response at the onset of conduction breakdown. The non-linearity is described (Nahm, 2006) by equation

$$I = KV^{\alpha} \quad (1)$$

Where k is a constant and α is the non-linearity coefficient, both of which are properties of the particular varistor material. Also the leakage current describes the current through the varistor in the pre-breakdown region (Bernik *et al.*, 2007; Leach *et al.*, 2000; Bernik *et al.*, 2008).

Varistors are useful as a shunt path for voltage surges arising from power transients (Anas *et al.*, 2007; Leach, 2005) thereby protecting sensitive electric circuits. They are made by sintering doped ZnO powder with additives of transition metal oxide such as Bi_2O_3. It has been proposed that the dopants responsible for varistor behavior are cations of large ionic radii with low solubility in ZnO at low temperature (Han *et al.*, 2002). The hcp structure of Zn hosts cation in octahedral interstices with cation to anion ratio in the range 0.732-0.414 (Barret *et al.*, 1973) Bi induces varistor behavior thus constituting a varistor former (Levinson *et al.*, 1986; Bernik *et al.*, 2001; Elfwing *et al.*, 2000). On the other hand, dopants like Co, Mn improve the non-ohmic properties and densification making them more stable and reliable. However the vaporization of Bi during processing makes Bi-doped varistor unstable (Xu *et al.* 2009).

Several authors have undertaken studies on varistor microstructure within the multicomponent system with very limited reports on the use of Pb and Mn . This work therefore has the objective of investigating the microstructural effect of binary doping with Mn and Pb in alternate proportions on the non-ohmic response. In a previous work (Akinnifesi *et al.*, 2012) involving the separate and combined doping of ZnO with Mn and Pb, the donor concentration contribution by Mn was found to be depressed by the presence of Pb. Kourdi *et al.*, (1992) reported that a bulk varistor consisted of several series and parallel microvaristors in which variation in characteristics was due to structure modification by dopant ions. Clarke (1999) observed that a thin intergranular phase separating grains gave rise to localized defects on the interface, leading to the presence of schottky barrier which limit current flow at low temperature. Mahan *et al.* (1979) proposed that a high value of the non-linearity coefficient was generated by the minority carrier creation in the schottky barrier region of the ZnO

grains. Consequently an application of high voltage ($V > V_T$) across the boundary layer produces conductivity increase by several orders of magnitude. In this way, the resistance of a varistor varies automatically in response to changes in the voltage level across the grains.

MATERIALS AND METHODS

Sample Preparation

Commercial grade specimen of ZnO, MnO_2 and PbO powders were procured and appropriate fractions of each component were weighed with a digital electronic balance of sensitivity 10^{-4} g. Following the procedures of direct mixing of constituent phases technique (Brankovic *et al.*, 2007), two sample types were constituted as A (95 mol % ZnO, 3 mol % PbO, 2 mol % MnO_2) and B (95 mol % ZnO, 2 mol % PbO, 3 mol % MnO_2). Each sample was thoroughly mixed and wet-milled in a pestle and mortar for several hours to obtain fine homogeneous particles. The mixture was calcinated in air at a temperature of 150°C for about 2 hours. A specimen of each sample was removed to a mould and compressed at a pressure of 2.5×10^{-2} N/m^2 into a disc form. Several discs were thus obtained and sintered between 750°C and 850°C for between 12 and 42 hours respectively as detailed in Table 1 for samples A1, A2, B1 and B2. This was an attempt to produce variation in microstructure. The sintering process was carried out in a quartz tube placed in an open-ended furnace which delivered heat at the rate of 5°C/min. The samples were allowed to cool in the oven to about 50°C. The final disc diameter and thickness were measured as 2.48 and 8.70×10^{-2} cm respectively.

Table 1: Details of Sample Description

Sample	Composition	Sintering Temperature	Sintering Time
A1	95% ZnO, 3% PbO, 2% MnO_2	800°C	12 hrs
A2	95% ZnO, 3% PbO, 2% MnO_2	850°C	18 hrs
B1	95% ZnO, 2% PbO, 3% MnO_2	750°C	42 hrs
B2	95% ZnO, 2% PbO, 3% MnO_2	850°C	36 hrs

Table 2: Non-ohmic Properties of the Varistor Samples .

Sample	Threshold Field, E_T (V/cm)	Leakage current J (μA/cm^2)	Non-linearity Coefficient a	Grain size (μm)
A1	13.5	1.52	0.32	2.075
A2	35.0	0.89	1.10	1.020
B1	17.0	0.54	1.60	2.200
B2	42.0	1.70	7.29	1.621

Sample Characterization

The microstructural details of the varistor samples were investigated with x-ray diffractometer of the type RADICON MD10 with Cuk_α radiation at 1.541 Å and a detection angle range between 16° and 72°. This revealed the crystal phases present in the varistor samples. The scanning electron microscopy of the samples gave clear images at 500X magnification as obtained with a CARL ZEISS SEM machine, mode EVOMA 10. From the images, grain sizes and distribution of phases were determined.

Information, about the threshold voltages, leakage current and non-linearity coefficient was obtained from the curves of DC electric field versus current

density (E-J) plots. For this purpose, the samples were provided with electrical leads on both surfaces by means of silver electrodes to establish ohmic contact. Measurements were made with a Keithley 2636A multi-meter.

RESULTS AND DISCUSSION

Microstructural Studies

The micrograph for sample A1 is shown in Figure 1a. This reveals grains that are spherical in nature with secondary phases scattered within the sample. This could have resulted from densification of the grains which are of average size 2.075 μm. Figure 1b shows the micrograph for sample A2. This consists of small grains and pores that are homogeneously distributed throughout the sample. The average grain size is 1.020 μm. Noting that sample A1 was sintered at a lower temperature and for a shorter duration than sample A2 with the same composition, it is obvious that microstructural modification arose from the sintering process. However grain growth may not proceed until sintering temperature reaches 800°C and over (Makovec *et al.*, 1993). The micrograph for sample B1 is shown in Figure 1c where the presence of a secondary phase and average grain size of 2.200 μm are observed. This could have been due to prolonged sintering time of 42 hours leading to grain growth in spite of the relatively low sintering temperature of 750°C. Figure 1d shows the micrograph for sample B2 with clear formation of large number of grains and different crystal phases. The average grain size is 1.62 μm. The microstructure appears more densified with the higher sintering temperature of 850°C. According to Nahm (2004), a more densified microstructure with reduced pores would accompany longer sintering time and higher sintering temperature.

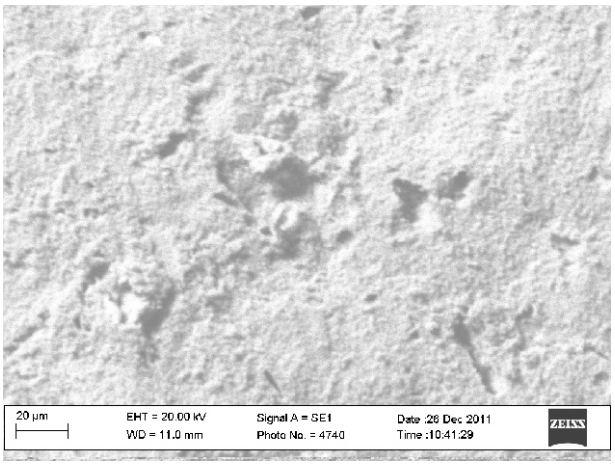

Figure 1a: Scanning Electron Micrograph of Sample A1

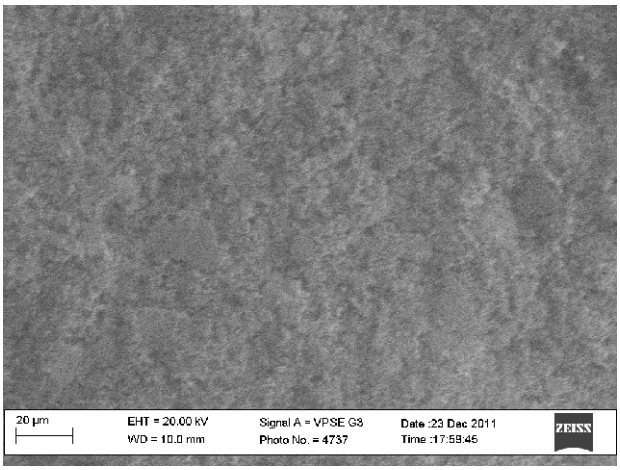

Figure 1b: Scanning Electron Micrograph of Sample A2

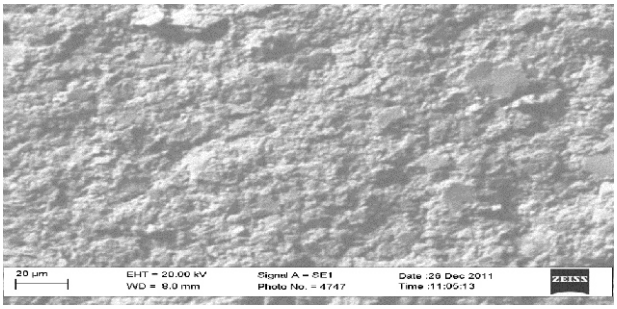

Figure 1c: Scanning Electron Micrograph of Sample B1

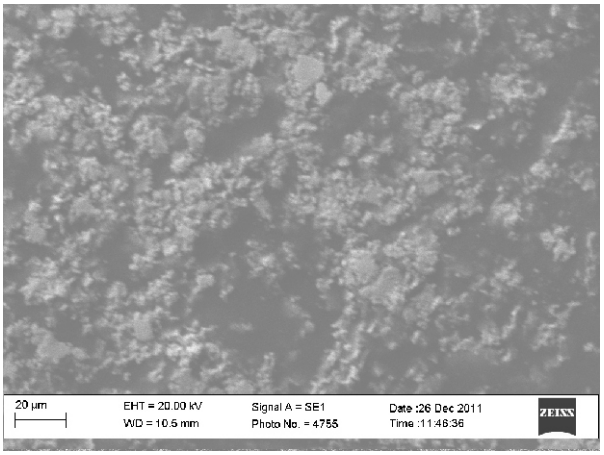

Figure 1d: Scanning Electron Micrograph of Sample B2

X-ray Diffraction Results

The loss of materials after sintering in the sample types A and B were respectively 19.69% and 14.09%. This could be explained by examining the XRD spectra of the samples as shown in Figures 2a-2d respectively. The formation of several secondary polymorphs of PbO and MnO_2 such as PbO_2 and Mn_5O_8 are indicated by prominent peaks in Figure 2a. Figure 2b reveals the formation of several secondary phases in the form of polymorphs also. As disappearance of pores would lead to densification, the loss of material would lead to decrease in densification.

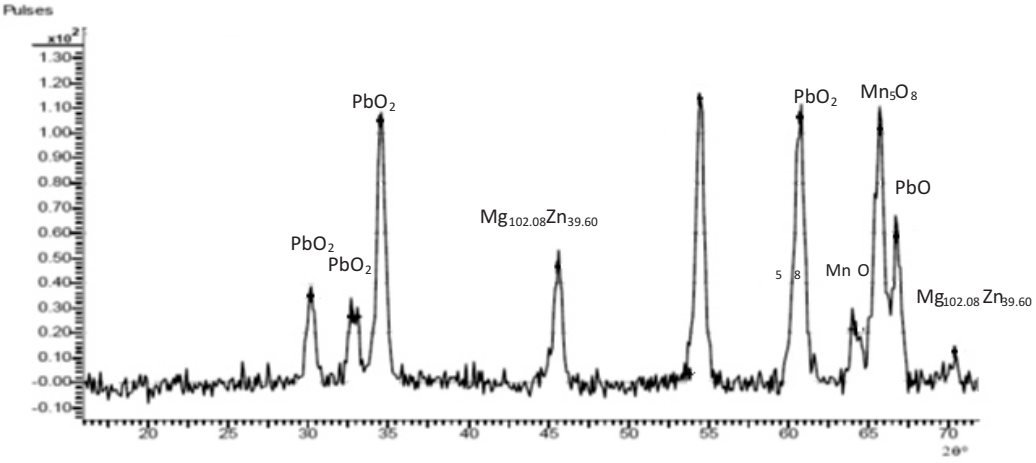

Figure 2a : XRD Spectrum of Sample A1

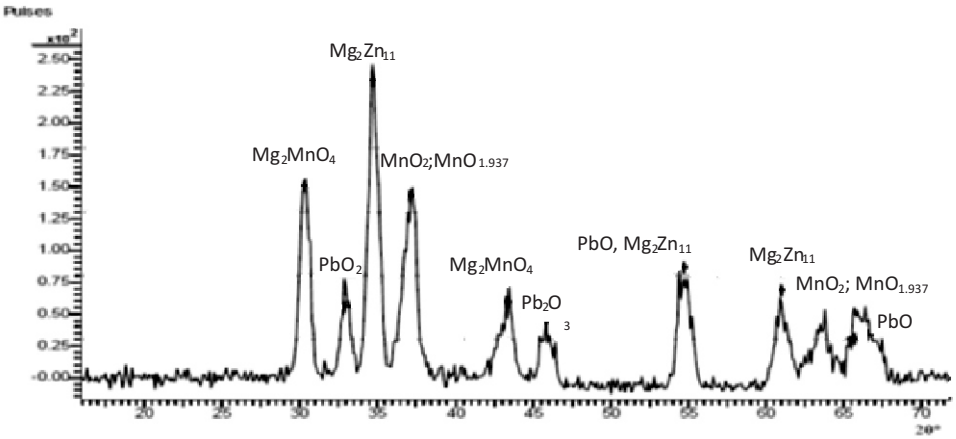

Figure 2b: XRD Spectrum of Sample A2

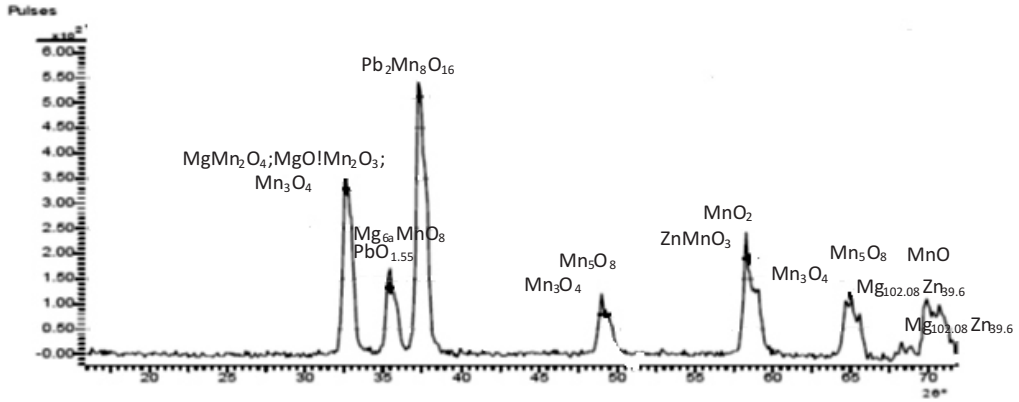

Figure 2c: XRD Spectrum of Sample B1

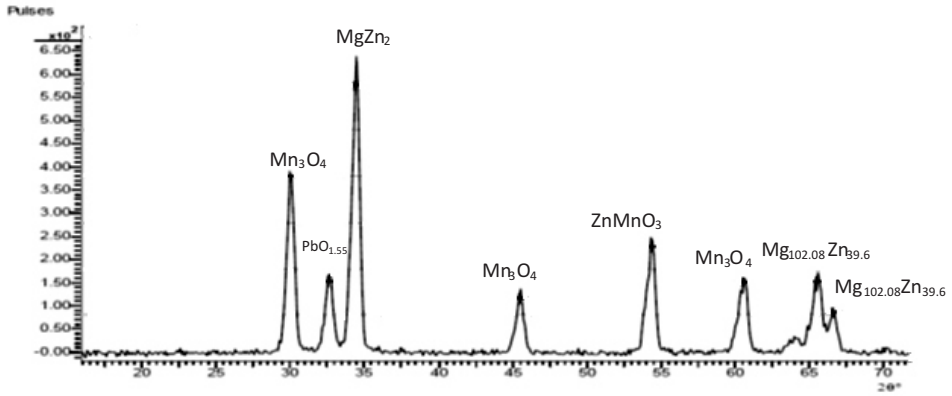

Figure 2d: XRD Spectrum of sample B2

Electrical Characterization

The measurements of current-voltage (E-J) response for sample A1, A2, B1 and B2 are plotted respectively in the Figures 3a-3d. These show a sharp transition from low current region to the non-linear region. The electrical conduction processes are distinct in the two regions, with the better varistor having a sharper transition. It is usual to relate current to voltage in varistors by equation (1). Taking the natural logarithm of this equation over the interval of the non-linearity gives α, the coefficient of non-linearity as

$$\alpha = \frac{Log\ J_L - Log\ J_N}{Log\ E_T - Log\ E_N} \qquad (2)$$

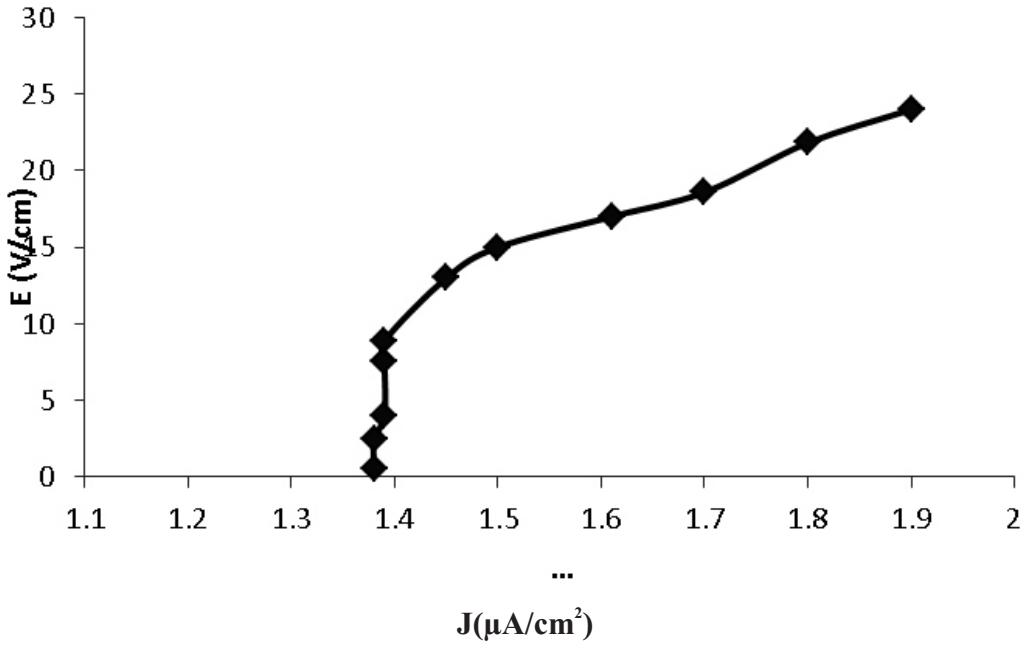

Figure 3a: Plot of Electric Field Against Current Density for Sample A1

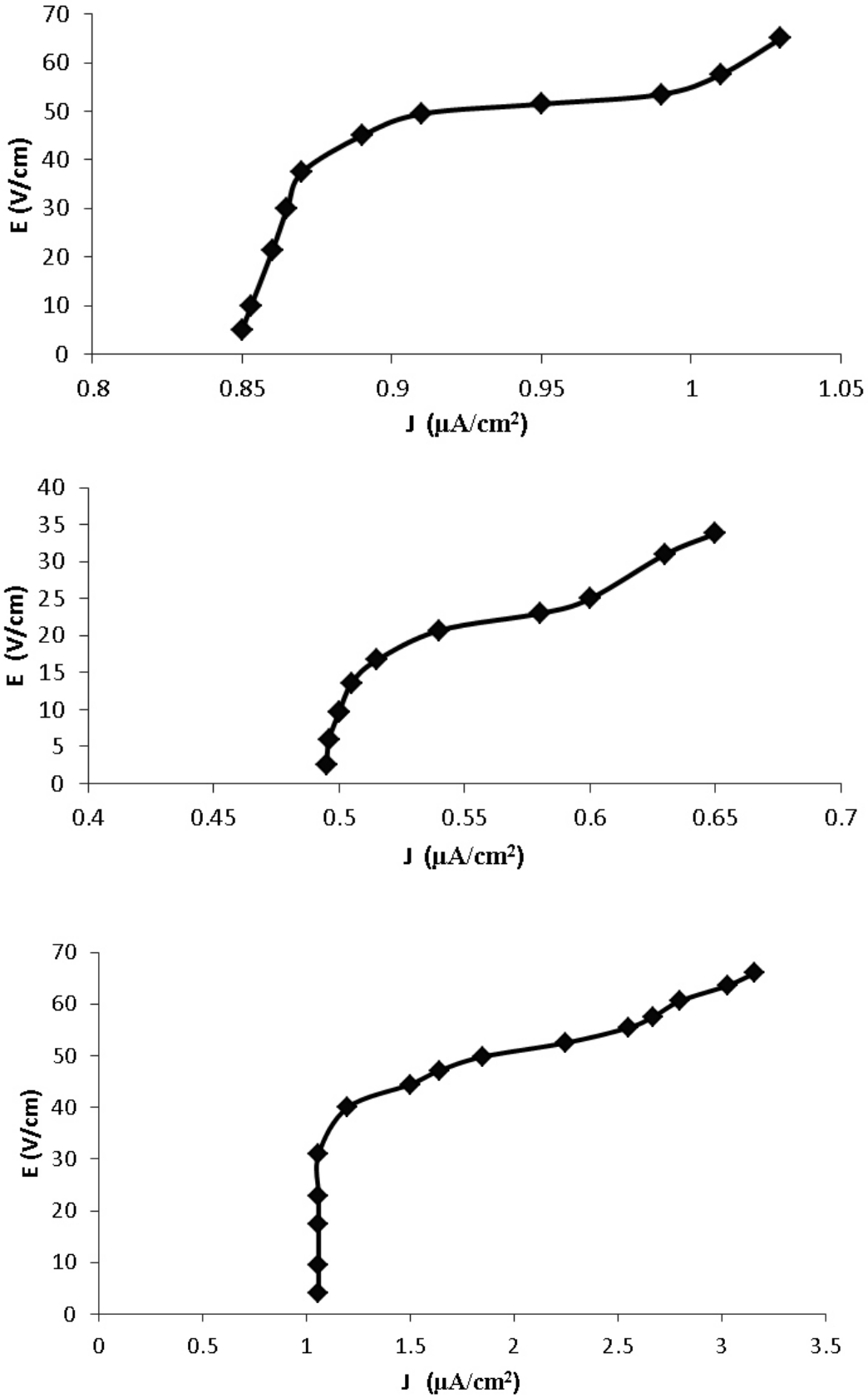

Figure 3d: Plot of Electric Field against Current Density for Sample B2

Similarly in A1 and A2 with lower Mn:Pb ratio, the breakdown fields are 13.5 and 35 V/cm respectively with α values of 0.32 and 1.10. Again sample A2 with a higher breakdown voltage was sintered with a higher temperature than sample A1 and for a longer time. The trend in both sample types A and B is that smaller grain sizes give rise to higher breakdown fields and coefficient of non-linearity, α in consistency with previous report by Xueya *et al.*, (2004). Large grains reduce the effective number of grain boundaries resulting in lower breakdown fields. Variation in non-ohmic properties relate to schottky barriers at grain boundaries (Nahm, 2007) and reduction in α corresponds to a lowering of barrier height (Leach *et al.*, 2000). Decreased leakage current, on the other hand, corresponds to a reduction in activation energy. The contribution to the barrier formation mechanisms by the migration of Zn interstitials to the grain boundaries takes place according to Frenkel reaction in the Zn sublattice (Han *et al.*, 2002).

$$Zn_i + V_{Zn} \Leftrightarrow Zn_{Zn} \quad (3)$$

However this can be moderated by the possibility of zinc interstitials annihilation in the bulk by gradual cooling, proceeding through the reaction.

$$Zn_i + \frac{1}{2} O_2(g) \Leftrightarrow ZnO \quad (4)$$

These mechanisms appear to feature remarkably in sample B2 with the highest non-linearity coefficient of 7.29 and breakdown voltage of 42 V/cm. The higher temperature of 850°C and longer time of 36 hours for the sintering process seem to have effectively shaped the microstructure of the sample.

CONCLUSION

The introduction of PbO and MnO_2 into zinc oxide ceramics in different ratios was carried out by direct mixing of constituent phases. The samples were sintered at different temperatures ranging from 750°C to 850°C for different lengths of time from 12 to 42 hours. This was done to obtain microstructural variations in the resulting varistor samples. Information about the phases, the densification and grain sizes and distribution in the microstructure were obtained by scanning electron micrograph and x-ray diffraction techniques. DC current-voltage characteristics were measured and analyzed through E-J plots. The formation of small and large grains and pores homogeneously distributed in the microstructure was revealed by the SEM images at 500X magnification. Evidence of grain growth and densification with high sintering temperature and extended sintering time was observed. The grain sizes ranged from 1.020 to 2.200 μm. Polymorphs of the constituent phases such as PbO_2 and Mn_5O_8 were identified from the XRD spectra. Some loss of materials in certain samples were determined and found traceable to the vaporization of MnO_2 .The E-J curves show a sharp transition from the electrically insulating state to the electrically conducting state with different characteristics, depending on the composition and fabrication of the samples. The non-ohmic properties such as the threshold and breakdown field, the leakage current and the coefficient of non-linearity were deduced from the E-J curves. These were found to depend on the grain sizes and other microstructural features of the samples. In general, lower grain sizes were found to be associated with higher breakdown field and non-linear coefficients. The variation of the non-ohmic properties was linked to the schottky barrier formation at the grain boundaries. The contribution of zinc ion interstitials migration to the grain boundary and the possibility of zinc interstitials annihilation in the bulk were proposed as possible mechanisms of the barrier control at the grain boundaries.

ACKNOWLEDGEMENT

The authors wish to acknowledge Sheda Science and Technology Complex, Abuja, Engineering Material Development Institute, Akure and Center for Energy Research and Development, Obafemi Awolowo University, Ile-Ife, for the use of their equipment.

REFERENCES

Akinnifesi, J. and Akinwunmi, O . 2012. Fabrication and electrical characterization of Zn-Mn-Pb oxide based varistors. Faculty of Science – International Conference Proceeding September 18 (unpublished)

Anas, S., Mangalaranja, R., Prothayal, M., Shukla, S. and Ananthakumar , S. 2007. Direct

sintering of varistor grade doped nanocrystalline ZnO and its densification through a step-sintering technique. *Acta Materialia* 55, 5792.

Barret, C., Nix, W. and Tetelman, A. 1973. The Principles of Engineering Materials Prentice Hall Inc. New Jersey, P.47.

Bernik, S., Mack, S. and Bui, A. 2001. Microstructural and electrical characteristics of Y_2O_3-doped ZnO-Bi_2O_3 based varistor ceramics. *Journal of the European Ceramic Society* 21, 1875

Bernik, S. and Daneu, N. 2007. Characteristics of ZnO-based varistor ceramics doped with Al_2O_3. *Journal of the European Ceramic Society* 27, 3161.

Bernik, S., Brankovic, G., Rustia, S., Zunic, M., Podlogar, M. and Brankovic, Z. 2008. Microstructural, compositional aspects of ZnO-based varistor ceramics prepared by direct mixing of the constituent phases and high energy milling. *Ceramics International* 34, 1495.

Brankovic, Z., Brankovic, G., Bernik, S., Zunic, M. 2007. ZnO varistors with reduced amount of additives prepared by direct mixing of constituent phases. *Journal of the European Ceramic Society* 27, 1101

Clarke, D. 1999. Varistor ceramics. *Journal of the American Ceramic Society* 82,485

Elfwing, M., Osterlund, P. and Olsson, E. 2000. Differences in wetting characteristics of Bi_2O_3 polymorphs in ZnO varistor materials . Journal of the American Ceramic Society 83, 2311.

Han, J., Senos, A. and Mantas, P. 2002. Varistor behavior of Mn-doped ZnO ceramics. *Journal of the European Ceramic Society* 22, 1653.

Kourdi, M., Bui, A., Loubierre, A. and Khedim, A. 1992. Behavior of metal oxide based varistors subjected to partial discharges in air . *Journal of Physics D : Applied Physics* 25, 548

Leach, C., Ling, z. and Frear, R. 2000. The effects of sintering temperature variations on the development of electrically active interfaces in zinc oxide based varistors. *Journal of the European Ceramic Society* 20, 2759

Leach, C. 2005. Grain boundary structures in zinc oxide variators. *Acta Materialia* 53, 237

Levinton, L. and Philipp, H. 1986 Zinc oxide varistors. A review. *American Ceramic Society* 28, 803

Mahan, G.D., Levinson, L. M. and Philipp, H. R. 1979. Theory of conduction in ZnO varistors. *Journal of Applied Physics*, 50, 2799-2812

Makovec, D., Kolar, D. and Trontelj, M. 1993. Sintering and Microstructural development of metal oxide varistor ceramics. *Materials Research Bulletin* 28 , 803

Nahm, C. 2004. Effects of sintering time on varistor properties of Dy_2O_3-doped ZnO . Pr_6O_4-based ceramics. *Materials Letters* 58, 3297

Nahm, C. 2006. Effect of sintering temperature on microstructure and electrical properties of Zn, Pr, Co, La oxide based varistors. *Materials Letters* 60, 3394

Nahm, C.W. 2007. Effect of sintering temperature on electrical properties and accelerated aging behavior of PCCL-doped ZnO varistors. *Materials Science and Engineering B*136 , 134

Xu, D., Shi, L., Wu, Z., Zhong, O. and Wu, X. 2009. Microstructure and electrical properties of ZnO-Bi_2O_3-based varistor ceramics by different sintering processes. *Journal of the European Ceramic Society* 29, 1789.

Xueya, K., Tu, M., Zhang, M. and Wang, T. 2004. Microstructure and electrical properties of doped zinc oxide varistor nano-materials. *Solid State Phenomena* 99, 127.